Synthesis and self-assembly of corona-functionalised polymeric arsenical nanoparticles

Hayden Tobin, Evelina Liarou, Ji-Inn Song, Alexandros Magiakos, Paul Wilson*

University of Warwick, Department of Chemistry, Coventry, CV4 7AL, UK

ABSTRACT

Polymeric arsenicals are emerging as an interesting platform for functional and (re)active materials in the field of polymer and (bio)materials science. Through exploiting the diverse and distinct reactivity of organic arsenicals in As(V), As(III) and As(I) oxidation states efficient methods for bioconjugation as well as hydrogel and nanoparticles formation have been reported. Here we expand on this body of work by reporting the synthesis of new amphiphilic block copolymeric arsenicals with a target composition of P((DMAm$_{100-X}$-*co*-AsAm$_X$)-*b*-DAAm$_{100}$) (**P1**, X = 0; **P2**, X = 5; **P3**, X = 20) which form nanoparticles (**NP1** – **NP3**; D_h = 49 - 71 nm) upon self-assembly in water. The mole fraction of the AsAm monomer appears to have an effect on the particle morphology and stability, with stability decreasing as a function of the AsAm mole fraction in the corona. The reactivity of the AsAm (As(V)) group has been exploited to modify the corona functionality via direct reduction (**NP$_{Red}$**) and sequential reduction and thiol substitution (**NP$_{GSH}$**). The resulting As(III)-functionalised nanoparticles (**NP$_{Red}$**) exhibited concentration-dependent toxicity against human prostate adenocarcinoma epithelia cell (PC-3) alluding to future development of these particles for mono- or combination therapy within appropriate nanoparticle formulations.

INTRODUCTION

The potential of organoarsenic polymers, referred to here as polymeric arsenicals, as functional polymers has been proposed for over 40 years.[1, 2] Synthetic strategies to produce polymeric arsenicals include; interfacial polycondensation reactions[3, 4] and ring-collapsed radical alternating copolymerization (RCRAC)[5], which results in the formation of backbone

functionalized polymeric arsenicals, whilst the use of vinyl-functionalised organic arsenical monomers[6] enables the formation side-chain functionalized polymeric arsenicals by free radical polymerization (FRP)[7, 8]. The proposed applications of these polymers have ranged from macromolecular therapeutics (anti-virals, anti-bacterials, anti-cancer)[9-14] to energy materials (semi-conducting, optics)[15, 16] to flocculants[17] and surfactants (for nanoparticle stabilization)[18, 19].

The clinical renaissance of (in)organic arsenicals, particularly organic arsenicals 4-(*N*-(*S*-glutathionylacetyl)amino) phenylarsonous acid (GSAO),[20] 4-(*N*-(*S*-penicillaminylacetyl)amino) phenylarsonous acid (PENAO),[21] that contain a common phenylarsonous acid (As(III)) group derived from commercial reagent *p*-arsanilic acid, has stimulated new interest in the potential of polymeric arsenicals as functional/(re)active platforms for bio(nano)materials design.[22] Over the last 5 years, the vinyl-functionalised organic arsenicals, previously employed in FRP, as well as arsenical-functionalised initiators have been employed for the synthesis of polymeric arsenicals via reversible deactivation radical polymerization (RDRP), furnishing side-chain and end-group functionalized polymeric arsenicals respectively.

Initially, an As(V)-functionalised α-bromoester initiator for Cu-mediated radical polymerisation was synthesized and employed in aqueous single electron transfer living radical polymerization (Aq-SET-LRP) to obtain As(V) chain-end functionalised (co)polymers[23]. Reduction of the As(V) end group to As(III) in the presence of glutathione promoted highly efficient and reversible conjugation *via* re-bridging of reduced disulfides. Subsequently, simple organic arsenical acrylamide monomers (AsAm), synthesised from *p*-arsanilic acid were employed in reversible addition fragmentation chain-transfer (RAFT) polymerization to afford (co)polymeric arsenical scaffolds that underwent efficient post-polymerization modification of

the pendent As(V) groups *via* sequential reduction (to As(III)) and thiol substitution in presence of a variety of organic and biologically relevant thiol reagents[24].

Aq-SET-LRP and RAFT have also been used to synthesize core-functionalised block copolymeric arsenicals capable of undergoing simultaneous thermally-induced self-assembly and reductive cross-linking. Considering the reactivity of the pendent As(V)-functional groups present in the block copolymers, three modes of cross-linking have been investigated. Firstly, reductive coupling, proceeding with the formation of As-As bonds, was achieved by heating the As(V)-functionalised block copolymers in the presence of hypophosphorus acid (H_3PO_2) and KI[25]. This strategy has also been used to prepare polymeric arsenical hydrogels stabilised by As-As bonds formed via reductive coupling[26]. In the second strategy, reductive coupling was performed in the presence of polythiol reagents to afford nanoparticles with greater stability with core cross-linking occurring through the formation more enthalpically favoured As-S bonds[27]. Most recently, nanoparticles have been prepared by sequential reductive and radical coupling occurring under the reductive conditions described above in the presence of the acetylenes. This results in the formation of nanoparticles stabilised by the formation of the vinylene-arsine cross-links within the core of the nanoparticles that are resistant to substitution (at the arsenic centre) and oxidative stress[28].

However, attempts to fabricate corona-functionalised particles using these strategies were unsuccessful as the particles formed upon heated were not stable due to insufficient number and/or proximity of cross-linking within the volume of the corona, leading to disassembly at room temperature.

Stenzel and co-workers have developed an alternative strategy for the formation of corona-functionalised polymeric arsenical nanoparticles. This involved multi-step synthesis of a PENAO-derived methacrylamide monomer followed by copolymerization of it into the

hydrophilic, corona-forming block of amphiphilic block copolymers via sequential polymerisation and then self-assembly.[29] A polymerisation induced self-assembly (PISA) strategy for polymeric arsenical nanoparticle formation has also been reported.[30] The PENAO-functionalised polymeric nanoparticles demonstrated improved activity and cell uptake of the particles relative to PENAO alone, with colocalization of the particles in mitochondria alluding to the potential for active targeting with organelle specificity.

Herein we report the synthesis of new amphiphilic block copolymeric arsenicals that have been used to prepare corona-functionalised polymeric arsenical nanoparticles. The resulting particles have been characterised with respect to the size and morphology and initial biological evaluation, via the XTT cell proliferation assay has been performed.

MATERIALS AND METHODS

N,*N*-Dimethylacrylamide (DMAm), diacetone acrylamide (DAAm), azobisisobutyronitrile (AIBN), trifluoroethanol, ascorbic acid, iodine solution, glycine, glutathione (GSH) and pyrene were purchased from Sigma-Aldrich and used as received. *N*-(4-(2,2,3,3,7,7,8,8-octamethyl-1,4,6,9-tetraoxa-5λ^5-arsaspiro[4.4]non-5-yl)-phenyl-2-propenamide) (AsAm(pin$_2$))[24] and 2-((butylthio)-carbonothioyl) thio propanoic acid (PABTC)[31] was synthesised according to the reported literature.

^{1}H NMR: spectra were recorded on a Bruker HD 300 spectrometer (300 MHz) where chemical shift values (δ) are reported in ppm relative to residual solvent peaks. ACDLABS software was used to analyse the data.

IR spectroscopy: IR transmission spectra were collected on a Bruker Alpha FT-IR spectrometer, scanning between a wavenumber of 400 and 4000 cm^{-1}. Data was analysed by Bruker's OPUS software.

DMF SEC (Mixed D column): Agilent Infinity II MDS instrument equipped with differential refractive index (DRI), viscometry (VS), dual angle light scatter (LS) and variable wavelength UV detectors. The system was equipped with 2 x PLgel Mixed D columns (300 x 7.5 mm) and a PLgel 5 µm guard column, made from poly(styrene divinylbenzene). The eluent is DMF with 5 mmol NH_4BF_4 additive. Samples were run at 1 ml.min^{-1} at 50'C. Poly(methyl methacrylate) standards (Agilent EasyVials) were used for calibration between 550 – 955,000 g.mol^{-1}. Analyte samples were filtered through a nylon membrane with 0.22 μm pore size before injection. Respectively, experimental molar mass ($M_{n,SEC}$) and dispersity ($Đ_m$) values of synthesized polymers were determined by conventional calibration using Agilent GPC/SEC software.

$CHCl_3$ SEC: Agilent Infinity II MDS instrument equipped with differential refractive index (DRI), viscometry (VS), dual angle light scatter (LS) and multiple wavelength UV detectors. The system was equipped with 2 x PLgel Mixed C columns (300 x 7.5 mm) and a PLgel 5 µm guard column, made from poly(styrene divinylbenzene). The eluent is $CHCl_3$ with 2 % TEA (triethylamine) additive. Samples were run at 1 ml.min^{-1} at 30'C. Poly(methyl methacrylate), and polystyrene standards (Agilent EasyVials) were used for calibration. Ethanol was added as a flow rate marker. Analyte samples were filtered through a GVHP membrane with 0.22 μm pore size before injection. Respectively, experimental molar mass ($M_{n,SEC}$) and dispersity ($Đ_m$) values of synthesized polymers were determined by conventional calibration using Agilent GPC/SEC software.

DLS: Size distributions were determined by DLS on a MALVERN Zetasizer Nano ZS operating at 25 °C with a 4 mW He-Ne 633 nm laser module. Measurements were made at a detection angle of 173° (back scattering). Measurements were repeated three times with

automatic attenuation selection and measurement position. The results were analysed using Malvern DTS 6.20 software.

Fluorescence spectroscopy: Emission spectra were measured using an Agilent Technologies Cary Eclipse Fluorescence spectrometer. The following conditions were adopted; PMT detector voltage 500 V, scan rate of 120 $nm.min^{-1}$, excitation slit width of 10 nm, emission slit width of 2.5 nm, emission wavelength range of 350-400 nm and pyrene excitation at 334 nm.

TEM: TEM images were recorded on a Jeol 2100 transmission electron microscope operated at 200 kV. Samples were prepared at 25 °C by drop-casting 7 µL of sample solution on copper grids with GO or formvar support. Excess solution was blotted away using filter paper and the drop casted TEM grid was left to dry for ~ 2 hours.

XTT cell proliferation assay: PC-3 cell-line (human prostate adenocarcinoma epithelia; ECACC 90112714) and NIH/3T3 cell-line (mouse embryonic fibroblasts; ECACC 93061524) were purchased from Sigma-Aldrich (UK) and cultured in Dulbecco's modified eagle media (DMEM) supplemented with 10% serum (foetal bovine serum for PC-3 and bovine calf serum for NIH/3T3, respectively), 2 mM glutamine and 1% penicillin (100 IU ml^{-1})/streptomycin (100 $\mu g ml^{-1}$) at 37°C in a 5% CO_2 humidified atmosphere in a cell incubator. Both cell-lines were routinely screened for mycoplasma infection using MycoAlert™ Mycoplasma Detection Kit (LT07-218; Lonza, US) as described in the instruction of the kit. No more than passage number 20 of each cell-line was used in this study.

For cell viability evaluation, PC-3 and NIH/3T3 cells were seeded in a flat-bottomed 96-well plate at a density of 5×10^3 cells in 100 µl per well. After 24 hours the culture medium was replaced by fresh media containing a series of dilution of the polymers, at the following concentrations: 8, 4, 2, 1, 0.5, and 0.25 $mg.ml^{-1}$. Prior to the serial dilution of the polymers, an

8 mg.ml^{-1} stock solution of each polymer was prepared by dissolving the polymers directly in cell culture medium and incubating for 1 hour at 37°C to ensure they were fully dissolved.

Following 24 hours incubation, the polymer containing medium was removed and each well was rinsed with PBS. The cells were incubated with 100 µl of a freshly prepared solution of XTT (0.25 mg.ml^{-1}) and N-methyl dibenzopyrazine methyl sulfate (1.88 µgml^{-1}) in the culture medium. After a 16-hour incubation absorbance of the wells was measured using a Cytation 3 plate reader (BioTek Instruments Inc., USA) at 450 nm (A450) and 650 nm (A650).

The relative cell growth relative to untreated control cells was calculated using the following formula:

$$Viability\ (\%) = \frac{(\mathrm{A450[Experimental]} - \mathrm{A450[Blank]} - \mathrm{A650[Experimental]})}{(\mathrm{A450[Control]} - \mathrm{A450[Blank]} - \mathrm{A650[Control]})} \times 100$$

The data presented are the mean ± standard deviation of two independent experiments where each sample was measured in triplicate.

Synthesis of P((DMAm$_{100\text{-}X}$-*co*-AsAm(pin)$_{2,X}$)-*b*-DAAm$_{100}$) (P1, P2p, P3p): DMAm (100-X eq), AsAm(pin)$_2$ (X eq, X = 0, 5, 20), CTA (23.8 mg, 0.100 mmol, 1 eq) and AIBN (1.64 mg, 10.0 µmol, 0.1 eq) were dissolved in TFE (3.97 ml) to create a 2 M solution (w.r.t. [M]$_{tot}$). The resulting solution was deoxygenated with nitrogen for 15 min before being heated at 65 °C overnight. The reactions were sampled for analysis by NMR and SEC. For chain extension, a separate solution of DAAm (100 eq) and AIBN (1.22 mg, 7.40 µmol) in TFE (2.00 ml) were deoxygenated with nitrogen for 15 min prior to addition to the reaction mixture. The resulting solution was heated at 65 °C overnight. The reactions were quenched by rapid cooling and exposure to air prior to precipitation in cold diethyl ether to afford the pure block copolymers **P1**, **P2p** and **P3p** as white solids.

Synthesis of P((DMAm$_{100-x}$-*co*-AsAm$_x$)-*b*-DAAm$_{100}$) (P2, P3): **P2p** and **P3p** (1 g) were separately dissolved in THF (25 mL). A 50% aqueous solution of HCl (25 mL) was added and the resulting mixture was stirred at room temperature for 24 hours. The reaction solutions were dialysed against MilliQ water over 3 days (nMWCO = 1 kD), changing the water twice per day. The pure polymers **P2** and **P3** were then isolated by lyophilisation.

Critical micelle concentration determination: A pyrene stock solution (0.202 mg ml^{-1}) in acetone was prepared. Aliquots of the stock solution (10.0 µl) were pipetted into glass vials, and the acetone was allowed to evaporate. Polymer solutions (**P1** – **P3**, 1.50 – 5.00x10^{-7} mg ml^{-1}) were prepared by serial dilution and added to the glass vials, resulting in a 2.00 µM concentration of pyrene in each sample. Each sample was loaded into a quartz cuvette for excitation and emission analysis via a fluorometer. The samples were excited at 334 nm (slit size 10.0 nm) and the emission intensity was collected between 350-470 nm (slit size 2.50 nm). I_1/I_3 was determined and plotted against $\log_{10}$(concentration) to determine the CMC at the point of inflection.

Formation of NP1 – NP3: Self-assembly was achieved by direct dissolution. Briefly, the deprotected polymers (**P1** – **P3**) were fully dissolved in MilliQ water (1.00 mg.ml^{-1}) with brief agitation using a bench-top vortex mixer, and then allowed to equilibrate at room temperature overnight prior to analysis by DLS and TEM.

Synthesis of NPX$_{Red}$: Solutions of **NP2** and **NP3** were prepared as described above. Ascorbic acid (10 eq w.r.t. AsAm) and iodine solution (1 eq w.r.t. AsAm) were added and the resulting solutions were stirred at room temperature for 18 hours. The purified particles **NP2$_{Red}$** and **NP3$_{Red}$** were purified by dialysis (nMWCO = 1 kD) against glycine (0.01 M) for 2 days, followed by MilliQ water for 3 days, with regular changing of the water, prior to isolation by lyophilisation.

Synthesis of NPX_{GSH}: Solutions of **NP2** and **NP3** were prepared as described above. Glutathione (10 eq w.r.t. AsAm) was added and the resulting solutions were stirred at room temperature for 18 hours. The purified particles **$NP2_{GSH}$** and **$NP3_{GSH}$** were purified by dialysis against MilliQ water (nMWCO = 1 kD) for 5 days, with regular changing of the water, prior to isolation by lyophilisation.

RESULTS AND DISCUSSION

Synthesis of arsenical-containing block copolymers (P1 – P3)

In order to synthesise corona-functionalised polymeric arsenical nanoparticles we adapted our previous strategies to target an amphiphilic block copolymer system comprised of a hydrophilic, corona-forming block of dimethylacrylamide (DMAm) and a hydrophobic core forming block of diacetone acrylamide (DAAm), which are well known form nanoparticles in polymerisation-induced self-assembly (PISA) formulations.[32-34] In order to incorporate the desired arsenical functional group into the corona forming block the organic arsenical acrylamide monomer (*N*-(4-(2,2,3,3,7,7,8,8-octamethyl-1,4,6,9-tetraoxa-5λ^5-arsaspiro[4.4]non-5-yl)-phenyl-2-propenamide; $AsAm(pin)_2$, was again synthesised according to our previous reports.[24] Due to the insolubility of the $AsAm(pin)_2$ monomer in water (deprotected after polymerisation, *vide infra*), PISA was not considered here. Alternatively, 2,2,2-trifluroethanol (TFE), which has previously been shown to be a good solvent for $AsAm(pin)_2$[27] was screened as a potential solvent for the solution polymerisation, with a view to performing self-assembly on the purified final block copolymers.

Initially, homopolymerisation of DMAm and DAAm by RAFT ($DP_{n,th}$ = 100) was performed to confirm compatibility with the TFE solvent system. Using AIBN as initiator and 2-(((butylthio)-carbonothioyl)thio)propanoic acid (PABTC) as CTA ([M] : [CTA] : [I] = [100] : [1] : [0.1]), PDMAm and PDAAm, were obtained with high conversion (> 99%) after stirring

at 65 °C for 23 hours. The structures of PDMAm and PDAAm were confirmed by ^{1}H NMR (Figure S1) while SEC revealed good agreement between theoretical ($M_{n,th}$) and experimental ($M_{n,SEC}$) number average molecular weight and low dispersity values (PDMAm $M_{n,th}$ = 10200 g.mol^{-1}, $M_{n,SEC}$ = 11900 g.mol^{-1}, $Đ_m$ = 1.17; DAAm; $M_{n,th}$ = 17200 g.mol^{-1}, $M_{n,SEC}$ = 14500 g.mol^{-1}, $Đ_m$ = 1.25, Figure S2).

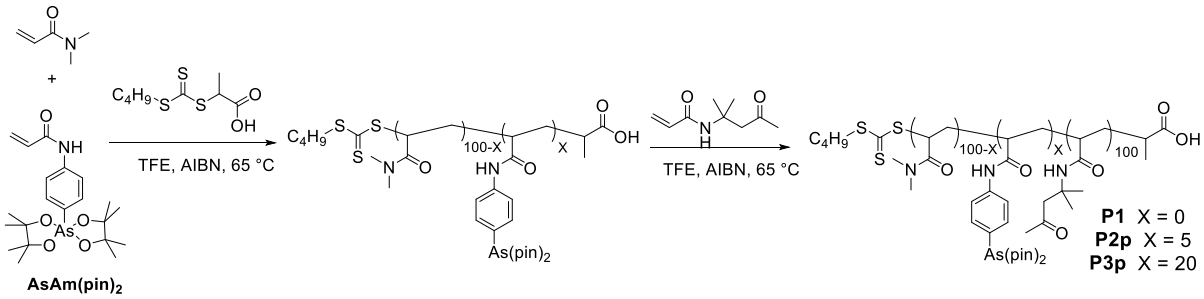

Scheme 1: Proposed reaction scheme for the synthesis of P((DMAm$_{100-X}$-*co*-AsAm(pin)$_{2,X}$)-*b*-DAAm$_{100}$) (**P1, P2p, P3p**) by RAFT polymerisation with *in situ* chain extension.

Amphiphilic block copolymers containing the pinacol-protected arsenic monomer AsAm(pin)$_2$, with a composition of P((DMAm$_{100-X}$-*co*-AsAm(pin)$_{2,X}$)-*b*-DAAm$_{100}$) (**P1, P2p, P3p**), were then targeted (Scheme 1). The mole fraction of the AsAm(pin)$_2$ monomer with respect to DMAm was varied (**P1**, X = 0; **P2p**, X = 5; **P3p**, X = 20) whilst employing stoichiometries of $[M]_{tot}$: $[CTA]_0$: [I] = [100] : [1] : [0.1] ($[M]_{tot}$ = 2 M)**.** For the synthesis of **P1**, DMAm was initially homopolymerised via RAFT using AIBN and PABTC again as the initiator and CTA respectively to form the hydrophilic, corona-forming macro-CTA. The reaction was followed by ^{1}H NMR and > 99 % conversion was obtained after stirring at 65 °C for 23 hours (Figure S3). For the preparation of **P2p** (X = 5) and **P3p** (X = 20), the corona-forming macro-CTA's were synthesised by initial copolymerisation of DMAm and AsAm(pin)$_2$ under the same conditions as **P1**. Integration of the vinyl peaks at 5.50-6.50 ppm revealed that the conversion, with respect to both monomers, reached > 99 % (Figure S4). The structure of the macro-CTA's was also confirmed by ^{1}H NMR through the presence of the aromatic protons at 7.50-8.20 ppm and methyl groups at 1.00 and 1.28 ppm of As(pin)$_2$ along

with the methyl protons arising from DMAm at 2.88 ppm (Figure S5). Molecular weight analysis of the macro-CTA's by SEC revealed $M_{n,SEC}$ between 11900 – 14,900 g.mol^{-1} and $Đ_m$ = 1.08 – 1.25, Table 1).

Table 1. Dispersity and number average molecular weight ($M_{n,SEC}$) for each synthesised polymer, before deprotection (calculated from SEC).

Target Polymer	X	Macro-CTA		Block Copolymer	
		$Đ_m$*	$M_{n,SEC}$* / gmol^{-1}	$Đ_m$*	$M_{n,SEC}$* / gmol^{-1}
P1	0	1.08	14,900	1.14	32,300
P2p	5	1.18	11,900	1.18	29,100
P3p	20	1.22	12,100	1.39	24,800

* Determined by SEC analysis using DMF as eluent

In situ chain extension of the PDMAm macro-CTA with DAAm was achieved by addition of DAAm (100 eq w.r.t. $[CTA]_0$) and supplementary AIBN to ensure sufficient radical concentration such that [DAAm] : $[CTA]_0$: [AIBN] = [100] : [1] : [0.1]. The resulting reaction was again followed by ^{1}H NMR and for the synthesis of **P1** > 99 % conversion was obtained after stirring at 65 °C for 23 hours according to integration of the vinyl peaks at 5.50-6.60 ppm and the CH_3 peak of PDAAm at 2.11 ppm (Figure 1A, S6). The conditions for chain extension were repeated using the macro-CTA's prepared for the synthesis of **P2p** and **P3p** respectively, reaching > 99 % conversion in both cases (Figure S7). Incorporation of DAAm into the block copolymers **P1, P2p** and **P3p** was confirmed by the appearance of the of the *gem*-dimethyl and methyl proton signals at 1.34 and 2.11 ppm respectively (Figure 1A). Qualitatively, the amount the $As(pin)_2$ increased with increasing mole fraction in the initial monomer feed. Unfortunately, the exact ratios could not be quantified due to a broad peak from the reaction solvent obscuring the broad DMAm methyl signals at 2.88 ppm. IR analysis also confirmed the presence of the $AsAm(pin)_2$ side-chains through the presence of the diagnostic As-O peaks at 950, 875 and 730 cm^{-1} the intensity of which increased as a function of the $AsAm(pin)_2$ mole

fraction (Figure 1B). SEC analysis revealed a shift in the molecular weight ($M_{n,SEC}$) to 24,800 – 32,300 g.mol^{-1} and a relatively low dispersity was retained upon chain extension and $Đ_m$ = 1.14 – 1.39 (Table 1, Figure 1C, Figure S8).

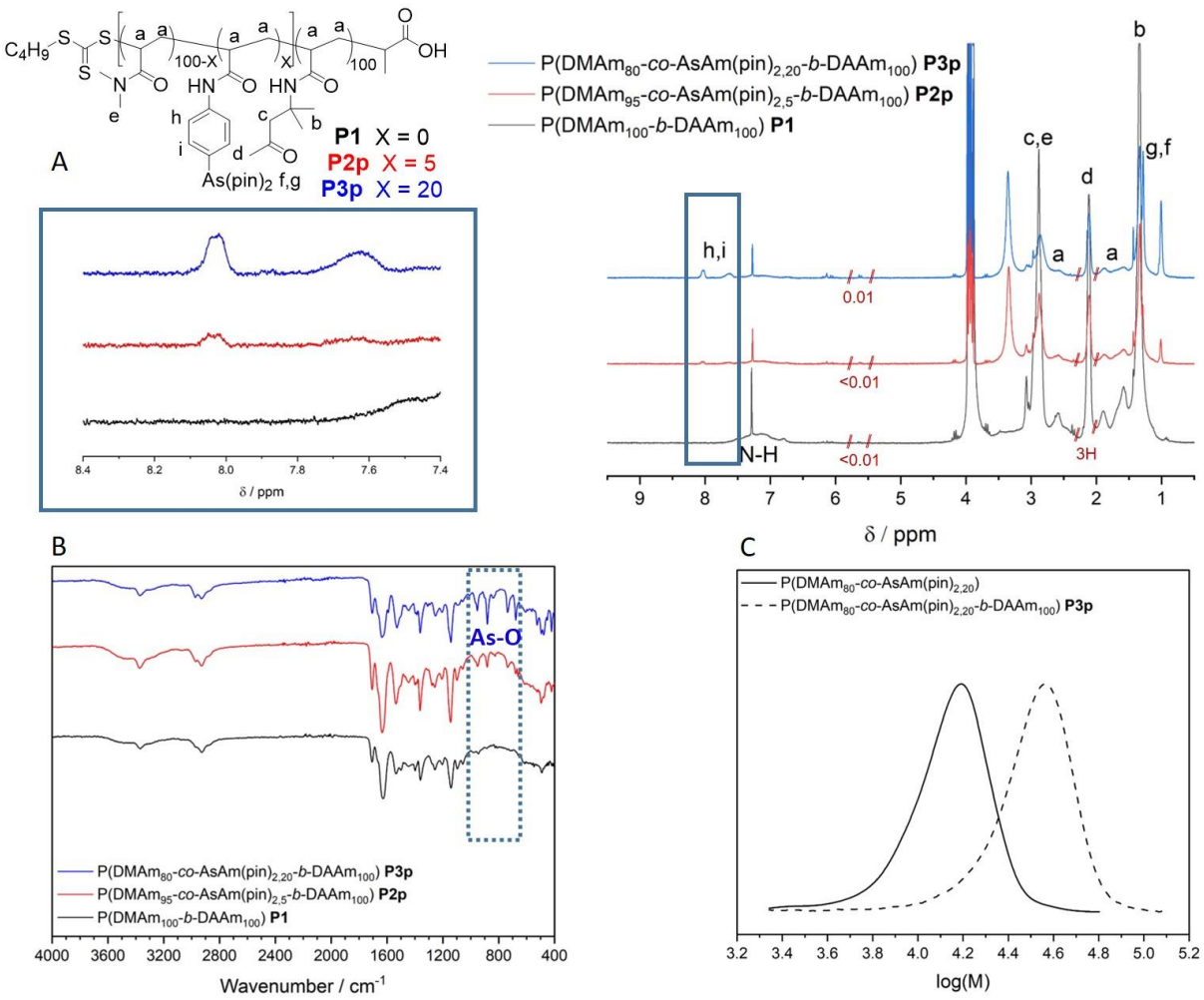

Figure 1. (A) ^{1}H NMR in $CDCl_3$ of **P1**, **P2p** and **P3p**. Incorporation of the DAAm monomer was confirmed by the appearance of the of the *gem*-dimethyl and methyl proton signals at 1.34 and 2.11 ppm respectively. Inset in blue shows enlarged spectra between 7.40 and 8.40 ppm showing the increase in the AsAm(pin)$_2$ aromatic signals incorporated into the polymers **P2p** and **P3p**. (B) Overlaid IR spectra of **P1**, **P2p** and **P3p** confirming the presence of the AsAm(pin)$_2$ groups with the increasing intensity of the As-O peaks at 950, 875 and 730 cm^{-1}. (C) Representative SEC (DMF) chromatogram confirming chain extension of the P(DMAm$_{80}$-*co*-AsAm(pin)$_{2,20}$ macro-CTA ($M_{n,SEC}$ = 12100 g.mol^{-1}, $Đ_m$ = 1.22) with DAAm to form the target block copolymer **P3p** ($M_{n,SEC}$ = 24800 g.mol^{-1}, $Đ_m$ = 1.39)

Finally, to obtain the desired arsenic acid (AsAm) functionalised polymers (**P2** and **P3**), the pinacol groups of the AsAm(pin)$_2$ side chain present in **P2p** and **P3p** were removed by stirring in THF containing 50% aqueous HCl. Successful removal of the pinacol groups was confirmed

by ^{1}H NMR by the absence of the methyl signals at 1.00 and 1.28 ppm respectively (Figure 2A). Retention of the proton signals corresponding to the DMAm, DAAm and AsAm side chain groups indicated that no deleterious sidechain reactions had occurred. Furthermore, IR showed that the As-O peaks had shifted to 920, 830 and 760 cm^{-1} respectively, whilst retaining the relative intensity as a functional of the AsAm side-chain (Figure 2B).

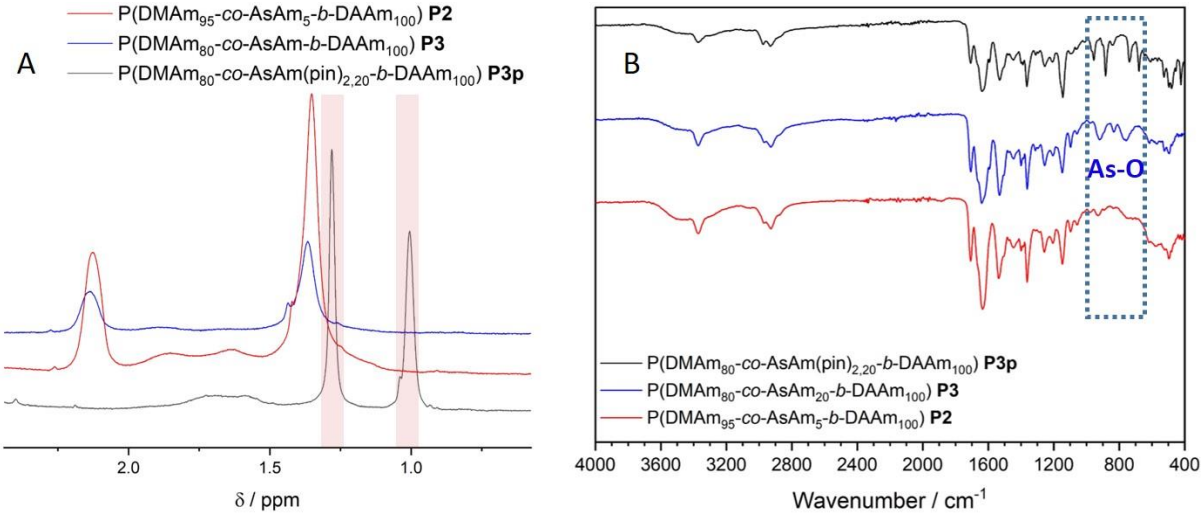

Figure 2. (A) ^{1}H NMR in $CDCl_3$ of **P2** and **P3** highlighting the successful removal of the $(pin)_2$ groups with the absence of the methyl signals at 1.00 and 1.28 ppm (representative peaks in **P3p** shown). (B) Overlaid IR spectra supporting the removal of the $(pin)_2$ groups through the shift in the As-O peaks to 920, 830 and 760 cm^{-1}.

Molecular weight analysis of **P2** by SEC (DMF solvent with 5 mM NH_4BF_4) showed the M_n value decreased significantly ($M_{n,SEC}$ = 16,700 g.mol^{-1}) while the dispersity increased ($Đ_m$ = 1.63) (Table S1). This unexpected change in the molecular weight and dispersity was attributed to the increased asymmetric nature of the molecular weight distribution, which showed increased tailing towards low molecular weight after deprotection (Figure S9). This suggested that converting the AsAm$(pin)_2$ side chain to AsAm had an effect on the hydrodynamic volume of the resulting polymers in DMF and led to interactions with the styrene-DVB stationary phase of the columns used. Analysis of **P2** by SEC using $CHCl_3$ (containing 2% triethylamine additive) before and after deprotection was therefore performed. The protected polymer containing the AsAm$(pin)_2$, **P2p**, gave $M_{n,SEC}$ of 19600 g.mol^{-1} and low dispersity values ($Đ_m$

= 1.18) (Table S1). Upon deprotection to yield the AsAm side chains, the M_n of **P2** again decreased more than expected ($M_{n,SEC}$ = 13,300 g.mol^{-1}) but the dispersity values were lower ($Đ_m$ = 1.28) due to less prominent tailing to low molecular weight (Figure S9). Molecular weight of **P3p** via SEC in $CHCl_3$ revealed an $M_{n,SEC}$ of 18,200 g.mol^{-1} and $Đ_m$ = 1.24 which after deprotection decreased to $M_{,SEC}$ = 13,300 g.mol^{-1} and $Đ_m$ = 1.10 (Figure S10). This data, together with the ^{1}H NMR and IR, which confirmed the presence of the key functional groups in the polymer side chains, suggest that the disparity observed in DMF SEC analysis for **P2** was an artefact of that particular solution properties of the deprotected polymers in that particular solvent system.

Self-assembly and formation of polymeric arsenical nanoparticles (NP1-NP3)

There are several different methods which can be utilised to form self-assembled structures from amphiphilic block copolymers, including direct dissolution, solvent switch, film re-hydration and nanoprecipitation.[35, 36] In this work, direct dissolution of the polymers in water was employed exploiting the amphiphilicity conferred by the hydrophilic DMAm-*co*-AsAm block and the hydrophobic DAAm block. Self-assembly was achieved by dispersing each polymer in water (1 mg.ml^{-1}) overnight at room temperature. The formation of nanoparticles (**NP1 – NP3**) was initially confirmed by dynamic light scattering (DLS), which revealed particles with hydrodynamic diameters (D_h) ranging from 49 – 71 nm (PDI = 0.071 – 0.28) (Figure 3).

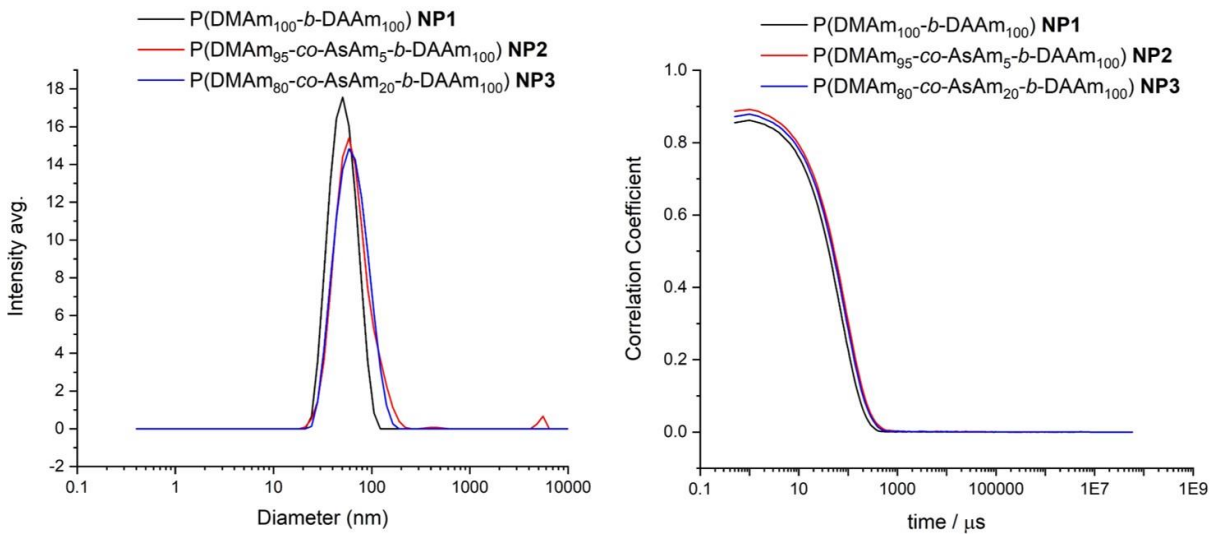

Figure 3. Particle size data from DLS Intensity measurements (H_2O, 1 mg.ml^{-1}) for **NP1** (D_h = 49 nm, PDI = 0.074), **NP2** (D_h = 71 nm, PDI = 0.28) and **NP3** (D_h = 57 nm, PDI = 0.16).

As DLS assumes spherical morphology, transmission electron microscopy (TEM) analysis was performed to gain an insight into the morphology of the nanoparticles formed. Previously, phase diagrams for aggregates assembled from block copolymers of DMAm and DAAm synthesised by PISA have been constructed. Armes *et al* showed that with relatively short stabilising blocks of DMAm (DP_n < 65) the morphology (0.1 wt% = 1 mg.ml^{-1}) changed from spheres to worms to vesicles as a function of increasing the DP_n of the DAAm block during the PISA process.[34] With longer stabilising blocks of DMAm (DP_n > 65), only spheres were observed irrespective of the DP_n of the DAAm block. Likewise, using DMAm as stabilising block and chain extending with mixture of DMAm and DAAm, Sumerlin *et al.* constructed a phase diagram as a function of the DP_n and DAAm feed ratio in a chain extension step.[33] In this work, with the stabilising DMAm block is $DP_{n,th}$ = 100, and chain extension with DAAm ($DP_{n,th}$ = 100, **NP1**), TEM (1 mg.ml^{-1}) indicated the formation of spherical aggregates with mean sphere diameters of ~ 15 nm (Figure 4A), which is consistent with the results of Armes *et al*. Interestingly, when AsAm was incorporated into the stabilising block (**NP2**) the presence of both spherical (diameters ~15 nm) and rod/worm-like (diameters ~15 nm, mean rod/worm length = 100-150 nm) aggregates were observed (Figure 4C). When the mole fraction of the

AsAm was increased further (**NP3**) a mixture of spheres and rod/worm-like aggregates with larger aspect ratios were observed (Figure 4C). Furthermore, when the concentration of the polymer containing the highest mole fraction of AsAm (**NP3**) was doubled (2 mg.ml^{-1}), TEM showed evidence of a transition to vesicular morphology, albeit in the presence of smaller spherical nanoparticles (Figure 4D). From the initial data, a tentative effect of the AsAm mole fraction in the corona on the morphology of the assembled structures is evident. The potential for ionisation and pH responsiveness of the arsenic acid group warrants further investigation and a systematic investigation into the structure-morphology relationship of this family of polymers is ongoing.

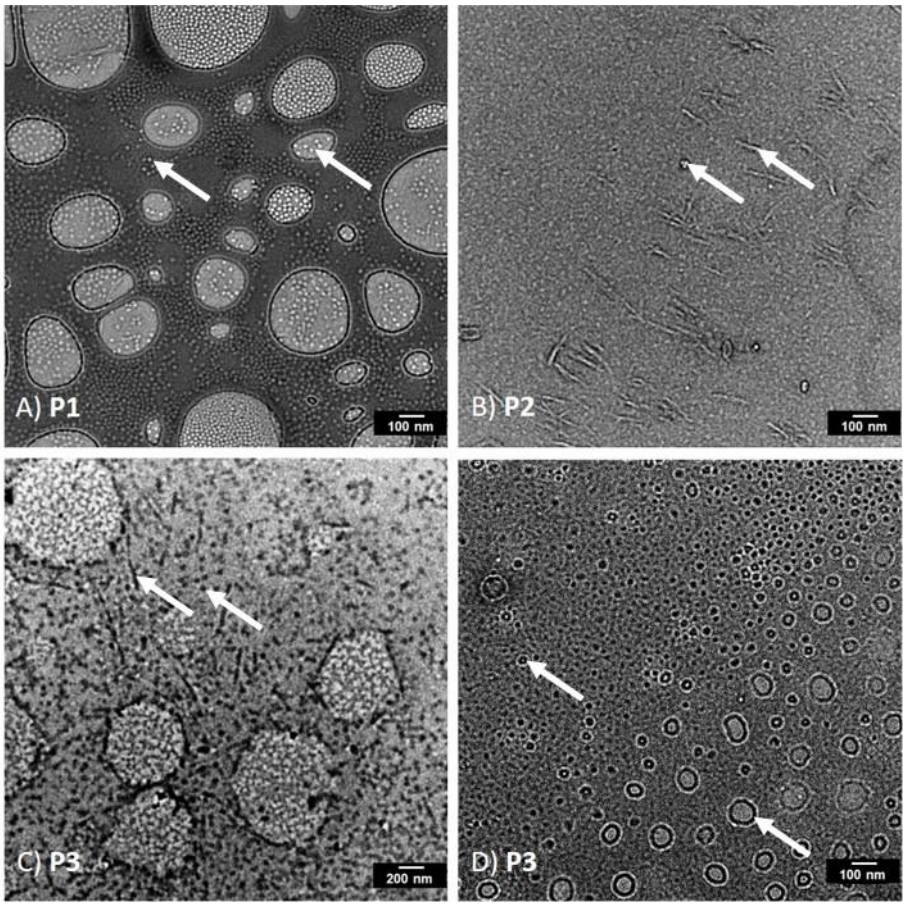

Figure 4. TEM imaging of (A) **NP1** (1 mg.ml^{-1}), spheres with mean diameters ~ 15 nm, scale bar 100 nm, arrows point to small features assigned as particles, larger features are artefacts of the grid. (B) **NP2** (1 mg.ml^{-1}), mixture of spheres (mean diameters ~15 nm) and rod/worm-like (diameters ~15 nm, mean rod/worm length = 100-150 nm), scale bar 100 nm, arrows point to small features assigned as particles. (C) **NP3** (1 mg.ml^{-1}), mixture of spheres and rod/worm-like, scale bar 200 nm, arrows point to small features assigned as particles, larger features are

artefacts of the grid. (D) **NP3** (2 mg.ml^{-1}) mixture of spheres and vesicles, scale bar 100 nm, arrows point to features assigned as particles.

To investigate the stability of the polymeric arsenical nanoparticles, the critical micelle concentration (CMC) was determined using the pyrene probe method as described in the literature.[37] Solutions of the polymers (**P1 – P3**) were prepared at concentrations of 2 mg.ml^{-1} which were then serially diluted to down to 5 x 10^{-7} mg.ml^{-1}. In all solutions the emission bands of the pyrene (2 µM) appeared as expected, allowing for the relative intensities of I_1 (372 nm) and I_3 (382 nm) bands, which change as a result of the pyrene environment, to be determined. The I_1/I_3 ratio values were determined and plotted as a function of concentration, with the CMC values being taken from the inflection point arising in these plots (Figure S11-S13). The polymer containing no AsAm (**P1**) had a CMC of 0.021 mg.ml^{-1} which is similar to PEO-based diblock copolymers and more stable than many low molecular weight surfactants.[38] Incorporation of AsAm into the corona-forming block led to the CMC increasing to 0.025 mg.ml^{-1} and 0.035 mg.ml^{-1} for **P2** and **P3** respectively. This is consistent with the observations of Stenzel *et al.* who prepared nanoparticles containing arsenical drug PENAO in the corona, attributing the decreased stability of the nanoparticles formed to ionisation of the arsenous acid pendant group leading the electrostatic repulsion between chains in the corona.[29, 30]

The biologically relevant oxidation states of the (in)organic arsenicals are As(V) and As(III).[39-42] We have been particularly interested in the formation of organic and polymeric arsenicals containing As(III) due to its high affinity for thiols which is implicated in its enhanced toxicity.[43, 44] As synthesised, **NP2** and **NP3** contain an arsenic acid (As(V)) group in their corona. Reduction of As(V) to As(III) can be achieved in a variety of ways. Treatment with reductants such as sulphur dioxide[45] or ascorbic acid,[46] can furnish arsenous acid (As(III)) groups upon work-up. Alternatively, reaction with an excess of monothiol reagents

has been show to proceed via two-electron reduction, from As(V) to As(III), followed by thiol addition to afford formation of dithio-arsines (As(III)).[47]

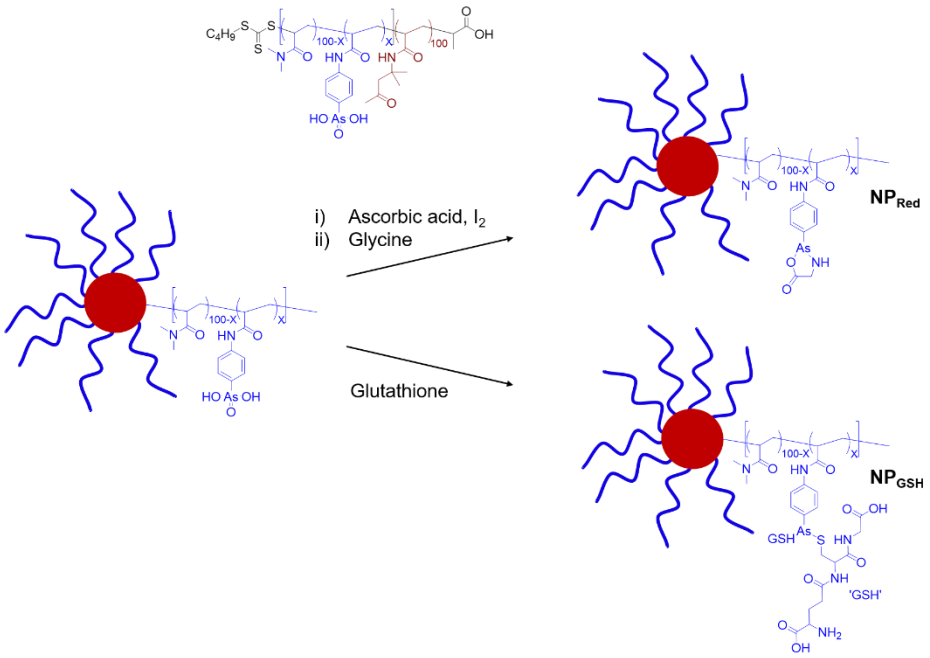

Scheme 2. Reaction scheme for the proposed modification of **NP2** and **NP3** reduced (**NP$_{Red}$**) and GSH modified (**NP$_{GSH}$**) nanoparticle structures.

To investigate the effect of arsenic oxidation state and modification on **NP2** and **NP3**, direct reduction, using ascorbic acid, and sequential reduction and substitution using tripeptide glutathione (GSH) was performed (Scheme 2). The arsenous acid (As(III)) functional groups obtained from direct reduction using ascorbic acid are oxidatively labile in aqueous solution. For enhanced stability the arsenous acid groups were trapped *in situ* using glycine as previously reported for related small molecule organic arsenicals.[45] The reduction reactions were confirmed by IR which showed significant changes in the As-O bonding region (600 – 950 cm^{-1}). Specifically, upon reduction by ascorbic acid, the diagnostic arsenic acid peaks at 922, 830 and 760 cm^{-1} were absent, with less intense peaks arising at 850 and 775 cm^{-1} assigned to the glycine-trapped arsenous acid group (As(III)) formed in **NP2$_{Red}$** (Figure S14) and **NP3$_{Red}$** (Figure 5A). Likewise, upon reaction with excess GSH the arsenic acid peaks were absent and a peak at ~ 870 cm^{-1} was observed, consistent with previous results[24] and indicative of the

formation of dithio-arsine functional groups in **NP2$_{GSH}$** (Figure S14) and **NP3$_{GSH}$** (Figure 5A). The reduction reactions had little effect of the nanoparticle size and distribution according to DLS with the resulting particles exhibiting D_h = 50 – 60 nm with PDI ~ 0.2 (Figure 5B).

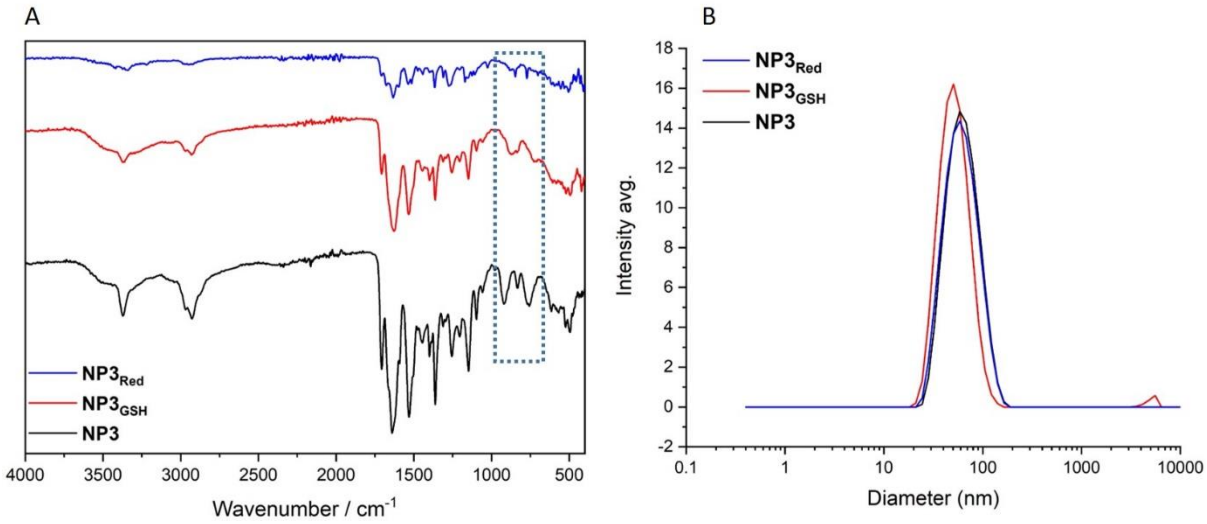

Figure 5. (A) Overlaid IR spectra supporting the modification of the **NP3** by reduction and sequential reduction and substitution by glutathione. Formation of **NP3$_{Red}$** and **NP3$_{GSH}$** respective was confirmed by the changes in the As-O bonding region (600 – 950 cm^{-1}). (B) Particle size data from DLS Intensity measurements (H_2O, 1 mg.ml^{-1}) for **NP3** (D_h = 57 nm, PDI = 0.16), **NP3$_{Red}$** (D_h = 55 nm, PDI = 0.17) and **NP3$_{GSH}$ (**D_h = 62 nm, PDI = 0.22).

Cell viability of NP1 – NP3

Preliminary cell viability of the corona-functionalised particles was assessed via the XTT cell proliferation assay using PC-3 (human prostate adenocarcinoma epithelia; ECACC 90112714) and NIH/3T3 (mouse embryonic fibroblasts; ECACC 93061524) cell-lines. The nanoparticles containing highest mole fraction of the AsAm (**NP3**) were evaluated over a concentration range of 0.25 – 8.00 mg.ml^{-1}. The viability of the As(V)-functionalised particles (**NP3**) remained high (>90 %) against both PC-3 and 3T3 cell-line up to 1 mg.ml^{-1} (Figure 6). The vialibility of 3T3 cells was found to decrease to ~75 % at very high particle concentrations (8 mg.ml^{-1}). A similar result was observed for the GSH-functionalised particles (**NP3$_{GSH}$**). Conversely, the As(III)-functionalised particles (**NP3$_{Red}$**) exhibited greater toxicity with viabilities decreasing significantly at high particle concentrations (> 1mg.ml^{-1}) to ~50 % and ~20 % for PC3 and 3T3

respectively. The greater toxicity **NP3$_{Red}$** compared to **NP3** is consistent with the understanding that As(III) (in)organic arsenicals are more toxic than the As(V) functionalised counterparts.[48]

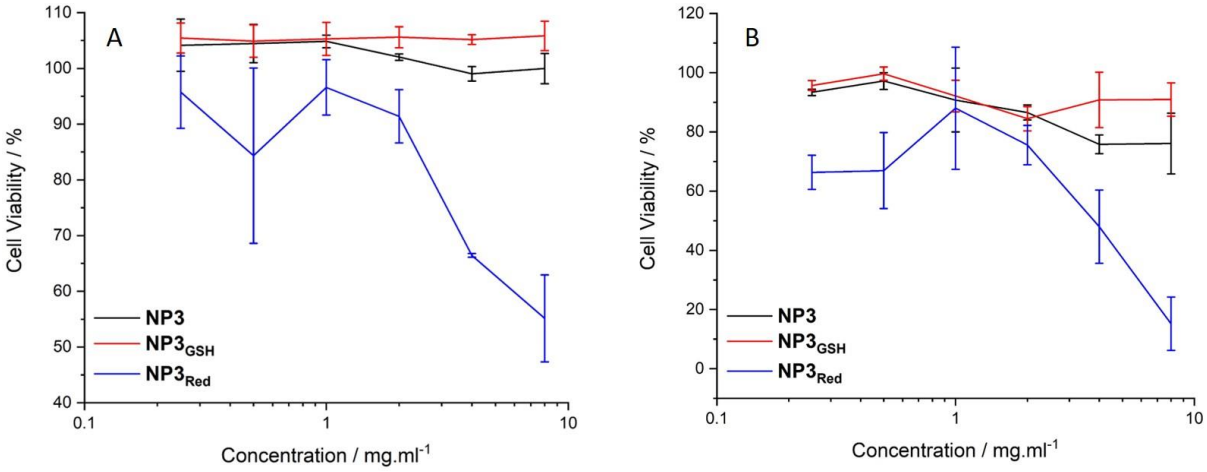

Figure 6. Preliminary cell viability data of the **NP3** nanoparticles measured using the XTT cell proliferation assay using (A) PC-3 (human prostate adenocarcinoma epithelia) and (B) NIH/3T3 (mouse embryonic fibroblasts) cell-lines. The data presented are the mean ± standard deviation of two independent experiments where each sample was measured in triplicate (Table S2, PC3; S3, 3T3).

Comparison of the viabilities of PC-3 and 3T3 cells **NP3$_{Red}$** suggest that there is no selectivity between healthy and cancerous cell-lines in the current formulation. This is unsurprising considering no specific targeting groups are present in the current nanoparticle formulation. The enhanced toxicity of **NP3$_{Red}$** is proposed to arise from the affinity of this As(III) group for thiol groups in the biological milieu, in particular at the mitochondria within cells.[49] This preliminary data therefore alludes to the potential of employing the corona-functionalised polymeric arsenical nanoparticles as mono- (response arising from the particles alone) or combination (response arising from the particles and loading the particles with therapeutics) therapies within formulations containing appropriate targeting ligands.

CONCLUSIONS

Amphiphilic block copolymeric arsenicals with a target composition of P((DMAm$_{100-X}$-*co*-AsAm$_X$)-*b*-DAAm$_{100}$), consisting of a hydrophobic core-forming block of DAAm and a hydrophilic corona-forming block of DMAm, containing increasing amounts of the As(V)-funcationalised monomer (AsAm; **P1**, X = 0; **P2**, X = 5; **P3**, X = 20), have been synthesised by RAFT polymerisation. The polymers undergo self-assembly by direct dissolution in MilliQ water to from stable nanoparticles (**NP1 – NP3**). The stability decreases slightly with increasing AsAm content (CMC = 0.021 – 0.035 mg.ml^{-1}), and changes in morphology have also been tentatively attributed to the AsAm content in the corona-forming block. The accessibility of the As(V) group in the corona of the nanoparticles lends itself to chemical manipulation which has been achieve by direct reduction (to As(III)) and sequential reduction and thiol substitution. Unlike our previously formulated, core-functionalised polymeric arsenical nanoparticles, the As(III)-corona functionalised nanoparticles exhibit a concentration-dependent cytotoxicity, which is in agreement with more complex PENAO-functionalised polymeric nanoparticles synthesised previously.[29][30] The data obtained with respect to the changes in nanoparticle morphology and cell viability as a function of the AsAm mole fraction in the corona of the nanoparticles distinguishes this work from our previous results and opens up new avenues of investigation which will support the development and enhance the potential of polymeric arsenicals as a functional, (re)active and responsive platform for (bio)materials science.

DATA AVAILABLITY

Additional data is presented in the supplementary information file. The raw/processed data from which this data was prepared is available upon request.

DECLARATION OF COMPETING INTERESTS

No conflicts of interest to report.

ACKNOWLEDGEMENTS

The authors would like to thank the Polymer Characterization and Microscopy Research Technology Platforms for maintenance, access and use of SEC, DLS and TEM facilities. P.W. thanks the Royal Society and Tata companies for the award of a University Research Fellowship (URF\R1\180274). A.M. thanks the EU Erasmus+ programme for funding a researcher mobility grant to visit Warwick and contribute to this project.

REFERENCES

[1] C.E. Carraher, W.G. Moon, Synthesis and initial characterization of arsenic (V) polyamines, Eur. Polym. J. 12(5) (1976) 329-331. https://doi.org/10.1016/0014-3057(76)90160-9
[2] L.R. Kallenbach, K.J. Irgolic, R.A. Zingaro, Organoarsenic polymers containing arsinic acid and arsenyl groups, Eur. Polym. J. 6(3) (1970) 479-485. https://doi.org/10.1016/0014-3057(70)90106-0
[3] C.E. Carraher, Production of organometallic polymers by the interfacial technique. I. Interfacial production of polyalkyloxysilanes and a study of some reaction variables, J. Polym. Sci., Part A-1: Polym. Chem. 7(8) (1969) 2351-2358. https://doi.org/10.1002/pol.1969.150070829
[4] C.E. Carraher, G.A. Scherubel, Production of organometallic polymers by the interfacial technique. XX. Synthesis of polyoxystannyloxyalkylenes, J. Polym. Sci., Part A-1: Polym. Chem. 9(4) (1971) 983-989. https://doi.org/10.1002/pol.1971.150090413
[5] K. Naka, T. Umeyama, Y. Chujo, Synthesis of Poly(vinylene-arsine)s: Alternating Radical Copolymerization of Arsenic Atomic Biradical Equivalent and Phenylacetylene, J. Am. Chem. Soc. 124(23) (2002) 6600-6603. https://doi.org/10.1021/ja026578l
[6] M.J. Percino, V.M. Chapela, R. Gutiérrez-Pérez, A.M. Herrera, New o- and p-methacryloylaminophenylarsonic monomers. Useful building units for water-soluble polymeric and nonlinear optical materials, Des. Monomers Polym. 3(2) (2000) 155-160. https://doi.org/10.1163/156855500300142843
[7] M.J. Percino, V.M. Chapela, A. Jiménez, Free radical polymerization kinetics of monomers functionalized with □AsO(OH)2 in aqueous media, J. Appl. Polym. Sci. 94(4) (2004) 1662-1669. https://doi.org/10.1002/app.20928
[8] B.A. Yáñez-Martínez, J. Percino, V.M. Chapela, Water-soluble copolymers from functionalized monomers (sodium o- and p-methacryloylaminophenylarsonate): Synthesis and characterization, J. Appl. Polym. Sci. 118(5) (2010) 2849-2858. https://doi.org/10.1002/app.32448
[9] C.E. Carraher, M.R. Roner, R. Thibodeau, A.M. Johnson, Synthesis, structural characterization, and preliminary cancer cell study results for poly(amine esters) derived from triphenyl-group VA organometallics and norfloxacin, Inorg. Chim. Acta 423 (2014) 123-131. https://doi.org/10.1016/j.ica.2014.07.004
[10] C.E. Carraher, M.R. Roner, M. Ayoub, N. Pham, A. Moric-Johnson, Synthesis and Preliminary Cancer Activity of Chelidonic Acid Polyesters Containing the Triphenylarsenic,

Triphenylantimony, and Triphenylbismuth Moiety, Int. J. Polym. Mater. Polym. Biomater. 64(6) (2015) 311-319. https://doi.org/10.1080/00914037.2014.945205
[11] C.E. Carraher, M.R. Roner, J. Dorestant, A. Moric-Johnson, M.H. Al-Huniti, Group VA Poly(amine esters) Containing the Antibacterial Ampicillin, J. Inorg. Organomet. Polym. Mater. 25(3) (2015) 400-410. https://doi.org/10.1007/s10904-014-0050-z
[12] C.E. Carraher, M.R. Roner, F. Mosca, A. Moric-Johnson, L.C. Miller, J.D. Einkauf, F. Russell, P. Slawek, Synthesis and Characterization, Including Cancer Cell Line Inhibition, of Group VA (Group 15)-Containing Polyesters from Reaction with Camphoric Acid, J. Inorg. Organomet. Polym. Mater. 27(6) (2017) 1627-1639. https://doi.org/10.1007/s10904-017-0622-9
[13] C.E. Carraher, M.R. Roner, N. Pham, A. Moric-Johnson, Group VA Polyesters Containing Thiodiglycolic Acid-Synthesis and Preliminary Cancer Activity, J. Macromol. Sci., Part A: Pure Appl.Chem. 51(7) (2014) 547-556. https://doi.org/10.1080/10601325.2014.916175
[14] C.E. Carraher, N.T.C. Truong, M.R. Roner, A. Moric, N.T. Trang, Synthesis of organoarsenic, organoantimony, and organobismuth poly(ether esters) from reaction with glycyrrhetinic acid and their preliminary activity against pancreatic cancer cell lines, J. Chin. Adv. Mater. Soc. 1(2) (2013) 134-150. https://doi.org/10.1080/22243682.2013.812281
[15] K. Naka, Y. Chujo, Organo-Arsenic, Phosphorus, and Antimony Conjugated Polymers, Conjugated Polymer Synthesis, Wiley-VCH Verlag GmbH & Co. KGaA2010, pp. 229-249. https://doi.org/10.1002/9783527632664.ch9
[16] A. Nakahashi, K. Naka, Y. Chujo, 1,4-Dihydro-1,4-diarsinine: Facile Synthesis via Nonvolatile Arsenic Intermediates by Radical Reactions, Organometallics 26(7) (2007) 1827-1830. https://doi.org/10.1021/om070080g
[17] T. Zayas, M.J. Percino, J. Cardoso, V.M. Chapela, Novel water-soluble polyelectrolytes with arsonic acid group for flocculation application, Polymer 41(14) (2000) 5505-5512. http://dx.doi.org/10.1016/S0032-3861(99)00718-1
[18] K. Naka, A. Nakahashi, M. Bravo, Y. Chujo, Synthesis of poly(vinylene-arsine)s-stabilized silver nanoparticles, Appl. Organomet. Chem. 24(8) (2010) 573-575. https://doi.org/10.1002/aoc.1611
[19] J. García-Serrano, U. Pal, A.M. Herrera, P. Salas, C. Ángeles-Chávez, One-Step "Green" Synthesis and Stabilization of Au and Ag Nanoparticles Using Ionic Polymers, Chem. Mater. 20(16) (2008) 5146-5153. https://doi.org/10.1021/cm703201d
[20] L. Horsley, J. Cummings, M. Middleton, T. Ward, A. Backen, A. Clamp, M. Dawson, H. Farmer, N. Fisher, G. Halbert, S. Halford, A. Harris, J. Hasan, P. Hogg, G. Kumaran, R. Little, G.J.M. Parker, P. Potter, M. Saunders, C. Roberts, D. Shaw, N. Smith, J. Smythe, A. Taylor, H. Turner, Y. Watson, C. Dive, G.C. Jayson, A phase 1 trial of intravenous 4-(N-(S-glutathionylacetyl)amino) phenylarsenoxide (GSAO) in patients with advanced solid tumours, Cancer Chemother. Pharmacol. 72(6) (2013) 1343-1352. http://dx.doi.org/10.1007/s00280-013-2320-9
[21] P.J. Dilda, S. Decollogne, L. Weerakoon, M.D. Norris, M. Haber, J.D. Allen, P.J. Hogg, Optimization of the Antitumor Efficacy of a Synthetic Mitochondrial Toxin by Increasing the Residence Time in the Cytosol, J. Med. Chem. 52(20) (2009) 6209-6216. https://doi.org/10.1021/jm9008339
[22] J. Tanaka, T.P. Davis, P. Wilson, Organic Arsenicals as Functional Motifs in Polymer and Biomaterials Science, Macromol. Rapid Commun. 39(19) (2018) 1800205. https://doi.org/10.1002/marc.201800205
[23] P. Wilson, A. Anastasaki, M.R. Owen, K. Kempe, D.M. Haddleton, S.K. Mann, A.P. Johnston, J.F. Quinn, M.R. Whittaker, P.J. Hogg, Organic arsenicals as efficient and highly specific linkers for protein/peptide–polymer conjugation, J. Am. Chem. Soc. 137(12) (2015) 4215-4222. https://doi.org/10.1021/jacs.5b01140

[24] C. Footman, P.A.J.M. de Jongh, J. Tanaka, R. Peltier, K. Kempe, T.P. Davis, P. Wilson, Thiol-reactive (co)polymer scaffolds comprising organic arsenical acrylamides, Chem. Commun. 53(60) (2017) 8447-8450. http://dx.doi.org/10.1039/C7CC03880A
[25] J. Tanaka, S. Tani, R. Peltier, E.H. Pilkington, A. Kerr, T.P. Davis, P. Wilson, Synthesis, aggregation and responsivity of block copolymers containing organic arsenicals, Polym. Chem. (2018). http://dx.doi.org/10.1039/C7PY01852E
[26] J. Tanaka, J.-I. Song, A.M. Lunn, R.A. Hand, S. Häkkinen, T.L. Schiller, S. Perrier, T.P. Davis, P. Wilson, Polymeric arsenicals as scaffolds for functional and responsive hydrogels, J. Mater. Chem. B 7(27) (2019) 4263-4271. http://dx.doi.org/10.1039/C8TB02569J
[27] J. Tanaka, G. Moriceau, A. Cook, A. Kerr, J. Zhang, R. Peltier, S. Perrier, T.P. Davis, P. Wilson, Tuning the Structure, Stability, and Responsivity of Polymeric Arsenical Nanoparticles Using Polythiol Cross-Linkers, Macromolecules 52(3) (2019) 992-1003. https://doi.org/10.1021/acs.macromol.8b02459
[28] J. Tanaka, A. Evans, P. Gurnani, A. Kerr, P. Wilson, Functionalisation and stabilisation of polymeric arsenical nanoparticles prepared by sequential reductive and radical cross-linking, Polym. Chem. 11(14) (2020) 2519-2531. http://dx.doi.org/10.1039/D0PY00229A
[29] J.-M. Noy, H. Lu, P.J. Hogg, J.-L. Yang, M. Stenzel, Direct Polymerization of the Arsenic Drug PENAO to Obtain Nanoparticles with High Thiol-Reactivity and Anti-Cancer Efficiency, Bioconjugate Chem. 29(2) (2018) 546-558. https://doi.org/10.1021/acs.bioconjchem.8b00032
[30] J.-M. Noy, C. Cao, M. Stenzel, Length of the Stabilizing Zwitterionic Poly(2-methacryloyloxyethyl phosphorycholine) Block Influences the Activity of the Conjugated Arsenic Drug in Drug-Directed Polymerization-Induced Self-Assembly Particles, ACS Macro Lett. 8(1) (2019) 57-63. https://doi.org/10.1021/acsmacrolett.8b00853
[31] C.J. Ferguson, R.J. Hughes, D. Nguyen, B.T.T. Pham, R.G. Gilbert, A.K. Serelis, C.H. Such, B.S. Hawkett, Ab Initio Emulsion Polymerization by RAFT-Controlled Self-Assembly, Macromolecules 38(6) (2005) 2191-2204. https://doi.org/10.1021/ma048787r
[32] X. Wang, J. Zhou, X. Lv, B. Zhang, Z. An, Temperature-Induced Morphological Transitions of Poly(dimethylacrylamide)–Poly(diacetone acrylamide) Block Copolymer Lamellae Synthesized via Aqueous Polymerization-Induced Self-Assembly, Macromolecules 50(18) (2017) 7222-7232. https://doi.org/10.1021/acs.macromol.7b01644
[33] C.A. Figg, R.N. Carmean, K.C. Bentz, S. Mukherjee, D.A. Savin, B.S. Sumerlin, Tuning Hydrophobicity To Program Block Copolymer Assemblies from the Inside Out, Macromolecules 50(3) (2017) 935-943. https://doi.org/10.1021/acs.macromol.6b02754
[34] S.J. Byard, M. Williams, B.E. McKenzie, A. Blanazs, S.P. Armes, Preparation and Cross-Linking of All-Acrylamide Diblock Copolymer Nano-Objects via Polymerization-Induced Self-Assembly in Aqueous Solution, Macromolecules 50(4) (2017) 1482-1493. https://doi.org/10.1021/acs.macromol.6b02643
[35] A. Blanazs, S.P. Armes, A.J. Ryan, Self-Assembled Block Copolymer Aggregates: From Micelles to Vesicles and their Biological Applications, Macromol. Rapid Commun. 30(4-5) (2009) 267-277. https://doi.org/10.1002/marc.200800713
[36] Y. Mai, A. Eisenberg, Self-assembly of block copolymers, Chem. Soc. Rev. 41(18) (2012) 5969-5985. http://dx.doi.org/10.1039/C2CS35115C
[37] A. Adharis, T. Ketelaar, A.G. Komarudin, K. Loos, Synthesis and Self-Assembly of Double-Hydrophilic and Amphiphilic Block Glycopolymers, Biomacromolecules 20(3) (2019) 1325-1333. https://doi.org/10.1021/acs.biomac.8b01713
[38] R. Gref, A. Domb, P. Quellec, T. Blunk, R.H. Müller, J.M. Verbavatz, R. Langer, The controlled intravenous delivery of drugs using PEG-coated sterically stabilized nanospheres, Adv. Drug Delivery Rev. 16(2) (1995) 215-233. https://doi.org/10.1016/0169-409X(95)00026-4

[39] S.-J. Chen, G.-B. Zhou, X.-W. Zhang, J.-H. Mao, H. de The, Z. Chen, From an old remedy to a magic bullet: molecular mechanisms underlying the therapeutic effects of arsenic in fighting leukemia, Blood (2011). https://doi.org/10.1182/blood-2010-11-283598
[40] P.J. Dilda, P.J. Hogg, Arsenical-based cancer drugs, Cancer Treat. Rev. 33(6) (2007) 542-564. https://doi.org/10.1016/j.ctrv.2007.05.001
[41] S. Shen, X.-F. Li, W.R. Cullen, M. Weinfeld, X.C. Le, Arsenic Binding to Proteins, Chem. Rev. 113(10) (2013) 7769-7792. https://doi.org/10.1021/cr300015c
[42] J.-X. Liu, G.-B. Zhou, S.-J. Chen, Z. Chen, Arsenic compounds: revived ancient remedies in the fight against human malignancies, Curr. Opin. Chem. Biol. 16(1) (2012) 92-98.
[43] V.P. Whittaker, An experimental investigation of the "ring hypothesis" of arsenical toxicity, Biochem. J. 41(1) (1947) 56-62. https://doi.org/10.1016/j.cbpa.2012.01.015
[44] A.M. Spuches, H.G. Kruszyna, A.M. Rich, D.E. Wilcox, Thermodynamics of the As(III)−Thiol Interaction: Arsenite and Monomethylarsenite Complexes with Glutathione, Dihydrolipoic Acid, and Other Thiol Ligands, Inorg. Chem. 44(8) (2005) 2964-2972. https://doi.org/10.1021/ic048694q
[45] N. Donoghue, P.T.W. Yam, X.-M. Jiang, P.J. Hogg, Presence of closely spaced protein thiols on the surface of mammalian cells, Prot. Sci. 9(12) (2000) 2436-2445. https://doi.org/10.1110/ps.9.12.2436
[46] D. Park, A.S. Don, T. Massamiri, A. Karwa, B. Warner, J. MacDonald, C. Hemenway, A. Naik, K.-T. Kuan, P.J. Dilda, J.W.H. Wong, K. Camphausen, L. Chinen, M. Dyszlewski, P.J. Hogg, Noninvasive Imaging of Cell Death Using an Hsp90 Ligand, J. Am. Chem. Soc. 133(9) (2011) 2832-2835. https://doi.org/10.1021/ja110226y
[47] E.A.H. Friedheim, Substituted 1,3,5-triazinyl-(6)-aminophenyl-arsenic compounds, Friedheim, Ernst A. H., United States Patent, US2422724 A, 1947.
[48] H.V. Aposhian, R.A. Zakharyan, M.D. Avram, M.J. Kopplin, M.L. Wollenberg, Oxidation and detoxification of trivalent arsenic species, Toxicol. Appl. Pharmacol. 193(1) (2003) 1-8. https://doi.org/10.1016/S0041-008X(03)00324-7
[49] D. Park, J. Chiu, G.G. Perrone, P.J. Dilda, P.J. Hogg, The tumour metabolism inhibitors GSAO and PENAO react with cysteines 57 and 257 of mitochondrial adenine nucleotide translocase, Cancer Cell Int. 12(1) (2012) 11-11. https://doi.org/10.1186/1475-2867-12-11